Polymer 51 (2010) 2049–2056

Contents lists available at ScienceDirect

Polymer

journal homepage: www.elsevier.com/locate/polymer

# USANS study of porosity and water content in sponge-like hydrogels

Morgan A. Iannuzzi [a], Roderick Reber III [a], Daniel M. Lentz [a], Jun Zhao [b], Lan Ma [b], Ronald C. Hedden [b,*]

[a] Department of Materials Science and Engineering, The Pennsylvania State University, University Park, PA 16802, USA
[b] Department of Chemical Engineering, Texas Tech University, Lubbock, TX 79409, USA

ARTICLE INFO

*Article history:*
Received 17 October 2009
Received in revised form
18 February 2010
Accepted 21 February 2010
Available online 1 March 2010

*Keywords:*
Hydrogels
Porous
USANS

ABSTRACT

Ultra small-angle neutron scattering (USANS) methods and equilibrium swelling measurements are combined to characterize correlation length, pore volume fraction, and gel-phase water content in sponge-like hydrogels. USANS invariant analysis is applied to poly(hydroxyethylmethacrylate) gels prepared with 40–80 vol. % of an extractable porogen. These gels are strongly opaque in the swollen state, but become transparent upon drying due to shrinkage or disappearance of the pores. The correlation length associated with porosity is measured by fitting USANS data to an appropriate scattering model. By combining swelling measurements with USANS invariant analysis, it is possible to determine the equilibrium volume fraction of pores and the concentration of water in the gel phase without performing contrast variation measurements.



## 1. Introduction

Hydrogels are water-swollen polymer networks that have been widely studied as biomedical [1], biomimetic [2], super-absorbent [3], and stimuli-responsive [4] materials, in addition to their uses in consumer applications such as contact lenses. Porosity can be engineered into hydrogels to achieve rapid changes in the macroscopic volume swelling ratio in response to environmental conditions; to control the rate of release of a drug or other chemical agent; or to mimic the structure and/or mass transfer characteristics of living tissue. Micrometer-scale porosity has been introduced into both ionic and non-ionic gels [5–14] by leaching of a porogen after crosslinking or by other methods, in order to induce ultra-fast swelling response upon immersion in good solvents [15–17] or in response to temperature [18–23]. In stimuli-responsive gels, the presence of porosity decreases the response time, allowing shrinkage or swelling of the material in as little as a few seconds [6,7].

Optimizing the swelling kinetics or stimuli-responsive properties of porous gels requires methods for characterization of both pore volume fraction and gel-phase water content. Due to the possibility that the pore phase volume fraction ($\phi_1$) may change during swelling, it is usually not possible to assume *affine* changes in the dimensions of the voids upon swelling/deswelling. A suitable theoretical framework relating $\phi_1$ to the equilibrium volume swelling ratio ($Q$) is lacking. Experimental methods are needed to calculate both water concentration within the gel phase and the volume fraction of porosity in the swollen state ($\phi_{1s}$).

This report examines interrelationships between equilibrium swelling, pore volume fraction, and gel phase water content in hydrogels that contain a significant volume fraction of micrometer-scale pores. An analytical description of the swelling of porous gels in a good solvent is developed, without assuming how the size or volume fraction of the pores changes during swelling. We then experimentally examine the swelling behavior of porous hydrogels having different pore volume fractions. Gels are prepared from lightly crosslinked poly(hydroxyethylmethacrylate), poly(HEMA), while the pore phase is generated by removal of a polymeric porogen (40–80 mass %) by extraction in water. A unique feature of these sponge-like gels is that the pores undergo drastic shrinkage or collapse in the dry state.

Information regarding the equilibrium pore size and volume fraction in the swollen state is obtained from ultra small-angle neutron scattering (USANS). The USANS measurements allow independent determination of the correlation lengths associated with porosity and with concentration fluctuations in the gel phase. USANS is applied to both swollen and dry gels to characterize the extent to which pores shrink during drying. Finally, a method is illustrated for determining both the volume fraction of pores and the water content of the gel phase, by combining scattering invariant analysis with equilibrium swelling data.

## 2. Experimental section

### 2.1. Gel synthesis

Gels were synthesized by thermally initiated free radical polymerization of a mixture of 2-hydroxyethylmethacrylate (HEMA),

* Corresponding author. Tel.: +1 806 742 3557.
*E-mail address:* ronald.hedden@ttu.edu (R.C. Hedden).

0032-3861/$ – see front matter © 2010 Elsevier Ltd. All rights reserved.
doi:10.1016/j.polymer.2010.02.034

ethylene glycol dimethacrylate (EGDMA), 2,2′-azobisisobutyronitrile (AIBN), and poly(ethylene glycol) (PEG) as porogen. No significant amount of water was present during crosslinking. A stock solution was first prepared from 99 mass % HEMA (Alfa Aesar, 97%) and 1 mass % EGDMA (Alfa Aesar, 98%). The HEMA contained 500 ppm 4-methoxyphenol as stabilizer, which was not removed prior to polymerization. The porogen was a linear PEG of nominal molar mass 8,000 g mol$^{-1}$ (Fluka). AIBN (98%) was obtained from Sigma–Aldrich. A typical gel was prepared by mixing the HEMA/EGDMA stock solution and PEG porogen with AIBN in a sealed 10 ml Teflon® vial (Cole Parmer, Inc.) at ambient temperature, followed by gradual heating to 65 °C with stirring. The concentration of AIBN was 1 mass % of the total mixture in all cases. Solutions became transparent upon heating due to dissolution of PEG in the methacrylate monomers, after which stirring was ceased. Each gel was allowed to cure at 65 °C for 2 days, during which time microphase separation occurred due to exclusion of PEG from the crosslinked polymer phase. The 65 °C cure temperature was sufficient to suppress crystallization of the PEG from solution during crosslinking without exceeding the boiling point of the HEMA monomer (67 °C). Compositions of samples prior to crosslinking are described in Table 1. A non-porous control sample (A-00, Table 1) was prepared by mixing HEMA, EGDMA, and AIBN without any PEG porogen. It was necessary to cure the control sample at 55 °C in order to eliminate bubbles that formed at 65 °C.

As polymerization proceeded at 65 °C, phase separation occurred due to partial or total immiscibility of the PEG with the newly formed crosslinked poly(HEMA) network. For a PEG mass fraction ($w_{PEG}$) of 0.4 or higher, conversion of HEMA and EGDMA monomers to a network proceeded rapidly enough such that a microphase-separated morphology was locked in by crosslinking. Gross phase separation was suppressed because the system reached the gel point before it could separate into two macroscopic layers. In contrast, gels containing $w_{PEG}$ of 0.2 or 0.3 separated into two distinct layers with differing turbidity before the gel point was reached. Samples having $w_{PEG} < 0.4$ were therefore not further studied due to obvious macroscopic inhomogeneity, but all other gels were macroscopically homogenous and were studied by USANS.

### 2.2. Extraction of porogen and drying

The PEG porogen was extracted by swelling the cured mixture in a comparatively large volume of deionized water. The PEG molecules, which have –$CH_2OH$ endgroups, are not expected to become chemically incorporated into the network, as they are unable to participate in the free radical polymerization reaction. Thus, quantitative extraction of the PEG should be possible. The water was replaced with fresh water each day for 5 days or until the mass of the swollen gel ($M_s$) reached an equilibrium value. $M_s$ was determined after patting the surface of the gel dry with a lint-free wiper. To prepare gels for USANS measurements, each gel was removed from $H_2O$ after extraction, patted dry, and immersed in $D_2O$ (99 atom % D, Sigma–Aldrich) for 24 h. The $D_2O$ was replaced with fresh $D_2O$ two additional times before conducting USANS experiments, to ensure removal of $H_2O$. Some gels were instead dried after extraction in $H_2O$. Drying was accomplished by placing the gel on aluminum foil for 2 days in air, followed by drying under vacuum in a dessicator over anhydrous $CaCl_2$ until the mass of the extracted gel reached an equilibrium value ($M_{ex}$). The soluble fraction ($w_{sol}$) of each gel was then determined by comparing the original, unextracted mass ($M_{unex}$) to $M_{ex}$.

$$w_{sol} = 1 - \frac{M_{ex}}{M_{unex}} \tag{1}$$

**Table 1**
Compositions of selected samples prior to polymerization.

| Sample | Mass (HEMA + EGDMA) (g stock solution) | Mass PEG (g) | Mass AIBN (g) | Cure Temp. (°C) |
|---|---|---|---|---|
| A-00 | 1.00 | 0.00 | 0.01 | 55 |
| E-40 | 0.60 | 0.40 | 0.01 | 65 |
| F-50 | 0.50 | 0.50 | 0.01 | 65 |
| G-60 | 0.40 | 0.60 | 0.01 | 65 |
| H-70 | 0.30 | 0.70 | 0.01 | 65 |
| I-80 | 0.20 | 0.80 | 0.01 | 65 |

### 2.3. Low-vacuum SEM

Scanning electron microscopy (SEM) images were obtained under low vacuum (50 Pa) for gels E-40, G-60, H-70, and I-80 using a Hitachi TM-1000 Tabletop Microscope. A freshly cleaved surface was generated by slicing the swollen gel with a razor blade. The wet gel was then placed under vacuum in the SEM sample chamber and imaged immediately. Images were recorded for the gels' surfaces in a partially hydrated state, as the samples began to lose water immediately upon being placed under vacuum.

### 2.4. USANS characterization

Ultra small-angle neutron scattering (USANS) measurements were performed at the National Institute of Standards and Technology Center for Neutron Research using the BT5 Perfect Crystal Diffractometer [24], which is a Bonse–Hart type instrument that can probe scattering vectors ($q$) as low as $3 \times 10^{-5}$ Å$^{-1}$. Samples selected for USANS analysis were free of bubbles and cracks, which can significantly affect the scattered intensity at the low end of the USANS q-range. Swollen gels were immersed in $D_2O$ and held between quartz windows in sealed sample cells having 4 mm path length. The thickness of swollen gels ranged from 2.0 to 4.0 mm, and the diameter irradiated by the beam was set by a 1/2″ Gd mask. Dry gels ranged in thickness from 0.5 to 2 mm and the irradiated area was set by either a 1/2″ or 1/4″ Gd mask. Empty cell scattering was measured for a cell containing only the quartz windows and an appropriate mask. The neutron wavelength was 2.4 Å. Sample thickness was measured carefully for determination of absolute scattering intensity for invariant analysis.

For all gels except I-80, the USANS scattering intensity, $I(q)$, was fitted to the Teubner–Strey (TS) model [25], which was originally developed to describe scattering from bicontinuous microemulsions. The dependence of scattering intensity on q is given by:

$$I(q)_{TS} = \frac{1}{a_2 + c_1 q^2 + c_2 q^4} + I_{inc} \tag{2}$$

In Eq. (2), $I_{inc}$ is the incoherent background scattering intensity. The fitting parameters $a_2$, $c_1$, and $c_2$ are related to the correlation length ($\xi_{TS}$) and the domain size ($d_{TS}$) according to Eqs. (3) and (4):

$$\xi_{TS} = \left(\frac{1}{2}\left(\frac{a_2}{c_2}\right)^{1/2} + \frac{1}{4}\left(\frac{c_1}{c_2}\right)\right)^{-1/2} \tag{3}$$

$$d_{TS} = 2\pi\left(\frac{1}{2}\left(\frac{a_2}{c_2}\right)^{1/2} - \frac{1}{4}\left(\frac{c_1}{c_2}\right)\right)^{-1/2} \tag{4}$$

The correlation length in the swollen porous gels is associated with concentration fluctuations within the gel phase, whereas the domain size is associated with the length scale of the porosity. The scattered intensity from gel I-80 was fitted to a sum of an Ornstein–Zernicke function and a Debye–Bueche function [26]:

$$I(q)_{OZ+DB} = \frac{A}{\left(1+\xi_{OZ}^2 q^2\right)} + \frac{B}{\left(1+\xi_{DB}^2 q^2\right)^2} \quad (5)$$

where $A$ and $B$ are scale factors, and $\xi_{OZ}$ and $\xi_{DB}$ are correlation lengths associated with the OZ and DB functions, respectively.

The incident neutron beam was slit-collimated with a full-width at half-maximum (FWHM) of the vertical $q$-resolution of $\Delta q_v = 0.117$ Å$^{-1}$. The slit-smeared intensity measured by USANS is related to the cross section expected for pinhole collimation, $I(q)$, by Eq. (6) [27]:

$$(I(q))_{USANS}^{smeared} = \frac{1}{\Delta q_v}\int_0^{\Delta q_v} I\left(q^2+u^2\right)\,du \quad (6)$$

The slit-smeared intensity measured by USANS can be corrected to mimic pinhole collimation by applying a numerical desmearing algorithm. Alternatively, the slit-smeared USANS data can be fitted directly to a smeared scattering model. The latter approach was preferred, and fits of USANS data to Eqs. (2) and (5) were made using the smeared models included in the SANS Analysis package v. 6.011 provided by the NIST Center for Neutron Research (NCNR).

## 3. Results and discussion

### 3.1. Theory

The swelling of a porous hydrogel cannot be assumed to be an affine deformation because the pore volume fraction may vary during swelling. A method is developed here to experimentally determine the volume fraction of water-filled pores ($\phi_{1s}$) and the volume fraction of water in the gel phase ($\phi_{w2}$) at equilibrium. Here, an approach is developed for calculating both quantities using a combination of gravimetric swelling data and USANS.

Consider a non-porous gel that is swollen to equilibrium in water. The *mass swelling ratio* for the non-porous gel is defined as

$${}^{Q}_{h} = \frac{M_s}{M_{ex}} \quad (7)$$

where $M_s$ and $M_{ex}$ are its swollen and dry extracted masses, respectively. The uptake of water in the non-porous gel is exclusively due to absorption of water into the gel phase, as no voids are present at the micrometer scale or larger. In a sponge-like gel containing a pore phase (1) and a gel phase (2), ${}^{Q}_{h}$ of the gel phase is defined in the same way, but $M_s$ of the gel phase cannot be measured gravimetrically due to the presence of water in the pore phase.

For the swollen porous gel, all pores are assumed to be filled by water, while the gel phase is assumed to be swollen to equilibrium. The equilibrium volume fraction of the pore phase is given by Eq. (8):

$$\phi_{1s} = \frac{V_1}{V_s} \quad (8)$$

where $V_1$ is the volume of the pore phase and $V_s$ is the total swollen volume of the entire gel including the pores. If $V_2$ is the volume of the gel phase, then

$$V_s = V_1 + V_2 = \frac{M_1}{\rho_{H_2O}} + \frac{M_2}{\rho_2} \quad (9)$$

where $M_1$ is the mass of the water in the pore phase, $\rho_{H_2O}$ is the mass density of water, $M_2$ is the total mass of the gel phase including water, and $\rho_2$ is the mass density of the gel phase. To apply Eq. (9) to experimental data, expressions are needed for $M_2$, $M_1$, and $\rho_2$, none of which are directly measurable. The equilibrium swelling of the gel phase is re-written in terms of the mass swelling ratio ${}^{Q}_{h}$:

$$M_2 = M_{exh}^{Q} \quad (10)$$

$M_{ex}$ can be determined by weighing the porous gel after drying. The mass of water inside the pore phases ($M_1$) is given by:

$$M_1 = M_s - M_{exh}^{Q} \quad (11)$$

Assuming the molar volume of water in the polymer matrix is approximately equal to its bulk value, the volume of the pore phase at equilibrium is given by:

$$V_1 = \frac{M_s - M_{exh}^{Q}}{\rho_{H_2O}} \quad (12)$$

Assuming additivity of the volumes of water and polymer, the volume of the gel phase ($V_2$) is estimated by adding the dry volume of the polymer and the volume of the water absorbed:

$$V_2 = \frac{M_{ex}}{\rho_p} + \frac{M_2 - M_{ex}}{\rho_{H_2O}} = \frac{M_{ex}}{\rho_p} + \frac{({}^{Q}_{h}-1)M_{ex}}{\rho_{H_2O}} \quad (13)$$

In Eq. (13), $\rho_p$ is the density of the polymer matrix in the dry state. The mass density of the gel phase can then be written

$$\rho_2 = \frac{M_2}{V_2} = \frac{M_2/M_{ex}}{V_2/M_{ex}} = \frac{{}^{Q}_{h}}{\left(1/\rho_p\right) + ({}^{Q}_{h}-1)/\rho_{H_2O}} \quad (14)$$

Substituting Eqs. (10), (11), and (14) into Eq. (9),

$$V_s = \frac{M_s - M_{exh}^{Q}}{\rho_{H_2O}} + M_{ex}\left(\frac{1}{\rho_p} + \frac{{}^{Q}_{h}-1}{\rho_{H_2O}}\right) \quad (15)$$

Substituting Eq. (12) for $V_1$ and Eq. (15) for $V_s$ into Eq. (8),

$$\phi_{1s} = \frac{M_s - M_{exh}^{Q}}{M_s + \left(\rho_{H_2O}M_{ex}/\rho_p\right) - M_{ex}} \quad (16)$$

Eq. (16) relates $\phi_{1s}$ in a porous gel to the directly measurable quantities $M_s$ and $M_{ex}$ and the unknown quantity ${}^{Q}_{h}$. It is possible to evaluate $\phi_{1s}$ from Eq. (16) directly if a reasonable value for ${}^{Q}_{h}$ is known. For example if a non-porous reference gel is available that has the same chemical composition and crosslink density as the porous gel, then ${}^{Q}_{h}$ for the reference gel can be evaluated gravimetrically and inserted into Eq. (16). However, for porous gels prepared with a large volume fraction of a porogen, it is usually not clear to what extent the porogen will affect the chemical composition and crosslink density of the gel phase. Therefore, additional information is needed to safely evaluate both ${}^{Q}_{h}$ and $\phi_{1s}$ by Eq. (16).

Complementary information regarding the gel phase composition at equilibrium in water can be obtained from neutron scattering measurements, either by contrast variation or by invariant analysis. The latter approach is pursued here. The porous gel is immersed in $D_2O$ rather than $H_2O$ to enhance neutron contrast between the pore phase and gel phase ($\Delta\rho_n^2$). Scattering data must be obtained over a wide enough $q$-range to permit determination of the scattering invariant. For pinhole-collimated scattering, the invariant is related to $I(q)$ by Eq. 17:

$$\text{Inv} = \int_0^{\infty} q^2 I(q)\,dq \quad (17)$$

Alternatively, the invariant may be determined from slit-smeared USANS data using Eq. (17b):

$$\mathrm{Inv} = \frac{1}{\Delta q_v}\int_0^\infty qI(q)^{\mathrm{smeared}}\mathrm{d}q \tag{17b}$$

Evaluation of Eq. (17) or (17b) from experimental data can be accomplished in part by numerical integration over the $q$-range of the measurement ($q_{\min} < q < q_{\max}$). However, if the coherent part of $I(q)$ has a non-negligible value outside of the measured $q$-range, extrapolation of the data to $q > q_{\max}$ and $q < q_{\min}$ is required to approximate the invariant. Here, we use the analytical expression for $I(q)$ determined from best fits to the scattering data to extrapolate to higher and lower $q$. The scattering model is assumed to accurately describe the scattering intensity outside the experimental $q$-range. The invariant is therefore evaluated by Eq. (17c):

$$\mathrm{Inv} = \int_0^{q_{\min}} q^2 I(q)^{\mathrm{fit}}\mathrm{d}q + \frac{1}{\Delta q_v}\int_{q_{\min}}^{q_{\max}} qI(q)^{\mathrm{smeared}}\mathrm{d}q + \int_{q_{\max}}^{\infty} q^2 I(q)^{\mathrm{fit}}\mathrm{d}q \tag{17c}$$

The first and third integrals in Eq. (17c) are evaluated by integration of (non-smeared) analytical expressions determined from best fits to the data, whereas the middle integral is evaluated by numerical integration of the (smeared) raw data. Note that only the coherent portion of $I(q)$ is included in each integrand in Eq. (17c); the incoherent background scattering ($I_{\mathrm{inc}}$) is omitted or subtracted from each integral.

The invariant is related to the neutron contrast factor between the gel phase and the pore phase ($\Delta\rho_n^2$) by Eq. (18):

$$\mathrm{Inv} = 2\pi^2\Delta\rho_n^2\phi_{1s}(1-\phi_{1s}) \tag{18}$$

The neutron contrast factor is related to the scattering length densities of the pore phase ($\mathrm{SLD}_1$) and gel phase ($\mathrm{SLD}_2$) by Eq. 19:

$$\Delta\rho_n^2 = (\mathrm{SLD}_1 - \mathrm{SLD}_2)^2 \tag{19}$$

In the swollen state, the pores are filled with pure $D_2O$, so $\mathrm{SLD}_{D2O} = \mathrm{SLD}_1 = 6.4\times10^{-6}\,\text{Å}^{-2}$. The mass swelling ratio of the gel phase in $D_2O$ is $\widehat{Q}_d$, equal to the total mass of the $D_2O$-swollen gel phase divided by its dry mass:

$$^{Q}_{d} = \frac{\phi_{w2}\rho_{D_2O} + (1-\phi_{w2})\rho_p}{\left(1-\phi_{w2}\right)\rho_p} \tag{20}$$

In Eq. (20), $\phi_{w2}$ is the volume fraction of solvent in the gel phase, and $\rho_{D_2O}$ is the mass density of the solvent, taken to be 1.11 g cm$^{-3}$ for $D_2O$. $\widehat{Q}_d$ differs from $^{Q}_{h}$ only by a density correction:

$$^{Q}_{h} = {}^{Q}_{d}\left(\rho_{H_2O}/\rho_{D_2O}\right) \tag{21}$$

The SLD of the gel phase is written in terms of the SLDs of the solvent ($\mathrm{SLD}_{D_2O}$) and dry polymer ($\mathrm{SLD}_p$):

$$\begin{aligned}\mathrm{SLD}_2 &= \mathrm{SLD}_{D_2O}\phi_{w2} + \mathrm{SLD}_p(1-\phi_{w2})\\ &= \mathrm{SLD}_p + \phi_{w2}\left(\mathrm{SLD}_{D_2O} - \mathrm{SLD}_p\right)\end{aligned} \tag{22}$$

Substitution of the above expression for $\mathrm{SLD}_2$ in Eq. (19) yields:

$$\Delta\rho_n^2 = \left(\mathrm{SLD}_{D_2O} - \mathrm{SLD}_p\right)^2(1-\phi_{w2})^2 \tag{23}$$

If Eq. (20) is solved for $\phi_{w2}$, substitution into Eq. (23) yields:

$$\Delta\rho_n^2 = \left(\frac{\rho_{D_2O}/\rho_p}{(\rho_{D_2O}/\rho_p) + (^{Q}_{d} - 1)}\right)^2\left(\mathrm{SLD}_{D_2O} - \mathrm{SLD}_p\right)^2 \tag{24}$$

Finally, the scattering invariant is given by Eq. (25):

$$\mathrm{Inv} = 2\pi^2\left(\frac{\rho_{D_2O}/\rho_p}{(\rho_{D_2O}/\rho_p) + (^{Q}_{d} - 1)}\right)^2\left(\mathrm{SLD}_{D_2O} - \mathrm{SLD}_p\right)^2\phi_{1s}(1-\phi_{1s}) \tag{25}$$

The experimentally determined scattering invariant (from evaluation of Eq. (17c)) is set equal to the right hand side of Eq. (25), leaving only $\widehat{Q}_d$ and $\phi_{1s}$ as unknowns. Eq. (16) (swelling) and Eq. (25) (USANS) are solved simultaneously to yield values for both quantities. (If swelling data were obtained in $H_2O$ rather than $D_2O$, Eq. (21) is used to interconvert between $\widehat{Q}_d$ and $^{Q}_{h}$.)

### 3.2. Influence of drying on porosity

After extraction of the PEG porogen, the appearance of the gels was compared in the wet state and in the dehydrated state after slow drying in air. At equilibrium in water, all gels were highly opaque, but after drying, the extracted gels were nearly transparent (Fig. 1). Gel A-00, which did not contain any PEG, was transparent both in the swollen state and after drying. All gels except A-00 contain significant micrometer-scale porosity in the water-swollen state. The opaque appearance of the porous gels arises from refractive index mismatch between the poly(HEMA) gel phase and the water-filled pore phase. The transparency of the dry, extracted gels may indicate either disappearance (collapse) of the pore phase, or shrinkage of the pores to small enough dimensions such that scattering of visible light becomes unnoticeable. Upon re-hydration in water, the (glassy) dried-out gels of thickness ~1.0 mm regain their opaque appearance within a few hours.

Removal of the PEG was verified gravimetrically by comparing the soluble fraction ($w_{sol}$) determined by Eq. (1) to the mass fraction of PEG in the solution prior to polymerization ($w_{PEG}$). Assuming the gel fraction of the crosslinked poly(HEMA) phase is close to 1.0, $w_{PEG}$ should be approximately equal to $w_{sol}$ when extraction of the PEG porogen is complete. Fig. 2 shows a plot of $w_{sol}$ vs. $w_{PEG}$, which verifies complete removal of the porogen. The measured value of $w_{sol}$ slightly exceeds the value of $w_{PEG}$ for some of the gels. The $w_{sol}$ of the non-porous sample A-00 was 0.019 (gel fraction = 0.981), so loss of some mass from the poly(HEMA) phase can occur. Loss of up to 1% of the gel's initial mass may also be attributed to loss of the AIBN initiator by thermal decomposition and/or extraction. The complete extraction of PEG from the gels within a few days suggests that the pores may be interconnected in the fully swollen state.

Gels were imaged by low-vacuum SEM in the hydrated state to confirm the presence of porosity. Because the gels began to lose

**Fig. 1.** Appearance of gel F-50 in the water-swollen state (left) and the dry, exctracted state (right).

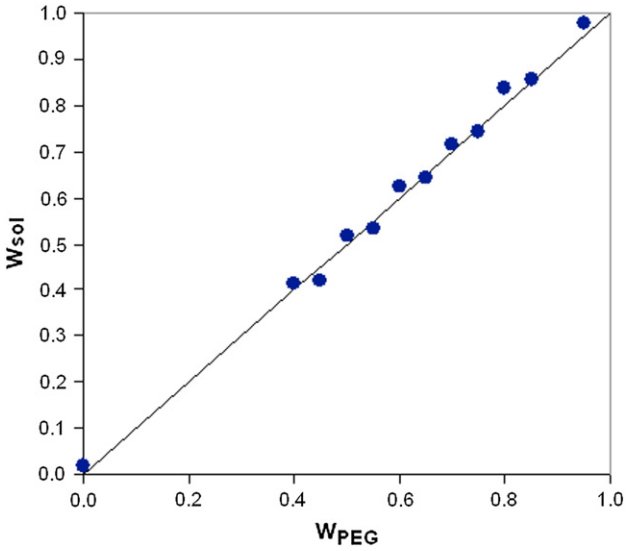


**Fig. 2.** Plot of soluble fraction ($w_{sol}$) determined by water extraction versus $w_{PEG}$, the mass fraction of PEG in the mixture prior to polymerization. The equation of the solid line is $w_{sol} = w_{PEG}$.

water as soon as they were placed under vacuum, the imaged surface is partially or totally dehydrated. (Although environmental SEM may be more appropriate, we did not have access to such instrumentation at the time of this study). Fig. 3(a) shows SEM images of the cleaved surfaces of four of the gels. Judging from the images, sample I-80 may have had the largest pores, whereas G-60 appeared to have had the smallest pores (in fact, no pores were resolved). Fig. 3 (b) shows a comparison of gel E-40 in the partially hydrated state and the air-dried state. Pores (dark regions) appear to be significantly more numerous in the hydrated state, which is consistent with the shrinkage or disappearance of pores after slow drying in air. Although the SEM images capture a qualitative picture of the pore morphology, the shrinkage of pores during drying frustrates quantitative analysis of pore size. In addition, SEM cannot determine the water content of the gel phase or the pore volume fraction, two quantities which are accessible through non-invasive USANS techniques.

### 3.3. USANS characterization: gels in $D_2O$

After complete extraction of the porogen, gels were studied by USANS in the swollen state in $D_2O$. Slit-smeared USANS data for several porous gels are presented in Fig. 4, for $3.4 \times 10^{-5}$ Å$^{-1}$ $< q <$ $2.66 \times 10^{-3}$ Å$^{-1}$. Data for gel F-50 were obtained over a wider $q$-range, up to $q = 9.43 \times 10^{-3}$ Å$^{-1}$, to examine the high-$q$ scattering power law. The non-porous gel A-00, though free of bubbles, could not be reliably characterized by USANS due to cracking of its surface during swelling in water or $D_2O$, which produced irreproducible scattering at the low end of the $q$-range. However, the porous gels did not crack and yielded reproducible scattering. Porous gels having $w_{PEG} < 0.8$ exhibited similar scattering characteristics: approximately constant $I(q)$ at low $q$, a very weak correlation peak near $q = 4.0 \times 10^{-4}$ Å$^{-1}$, and a rapid decay of scattered intensity at high $q$. The scattering from gel I-80, in contrast, exhibited an upturn in $I(q)$ at low $q$.

From the slit-smeared USANS data, the high-$q$ power law for gel F-50 was determined to be $3.06 \pm 0.07$ by a power law fit to the last 20 data points in Fig. 4 (the quoted uncertainty is the standard error in the slope). A high-$q$ power law of $I(q) \sim q^{-4}$ is expected for a two-phase system having sharp interfaces (Porod Law) for pinhole collimation, whereas a high-$q$ power law of $I(q) \sim q^{-3}$ would be expected for slit-smeared data. Gel F-50 is therefore assumed to have well-defined interphase boundaries. The other porous gels were assumed to exhibit similar a high-$q$ power law behavior, except I-80.

For the gels having $w_{PEG} < 0.8$, the scattered intensity was fitted to the Teubner–Strey (TS) model (Eq. (2)), which was originally developed to describe scattering from bicontinuous microemulsions. Although other models were also examined, only the TS model produced satisfactory fits to the high-$q$ portion of the scattering data. Although the TS model has not previously been applied to describe scattering from porous gels to our knowledge, it is assumed to be appropriate for porous gels with bicontinous structure (interconnected pores) and sharp interphase boundaries. Fig. 5 shows the best fit to the TS model for gel F-50. Fits to the data for E-40, G-60, and H-70 were of similar quality. It is possible that the microphase separation in the PEG-poly(HEMA) blends during polymerization generated morphology similar to a bicontinuous oil-water microemulsion, even though no surfactant was present in the gel formulation. The TS model is capable of generating a correlation peak, as is often observed in the scattered intensity from microemulsions, by setting the parameters $c_1$ positive and $c_2$ negative. For the porous gels in this study, which did exhibit a weak correlation peak in their scattering, no satisfactory fits to the data could be obtained with negative $c_2$ values, however. The only fits that adequately captured the high-$q$ decay of intensity were obtained with positive values of both $c_1$ and $c_2$. Fitting parameters determined by non-linear least squares analysis are summarized in Table 2.

The value of $\xi_{TS}$ is associated with concentration fluctuations in the gel phase, whereas $d_{TS}$ is taken to be an average grain size in the material, assumed to be of the same length scale as the average pore diameter. Interestingly, the largest $d_{TS}$ was found for gel E-40, which had the lowest mass fraction of PEG during crosslinking. The trend in pore size with decreasing PEG content is consistent with the approach to gross phase separation observed in samples having $w_{PEG} = 0.2$ or 0.3, and consistent with the SEM images. The magnitude of $\xi_{TS}$ is similar for all of the gels listed in Table 2.

The scattering from swollen gel I-80 differed markedly from that of the other gels. The upturn in scattering intensity at low $q$ is attributed to formation of a separate population of comparatively large pores or cracks during crosslinking. The shape scattering data cannot be captured by the TS model due to the low-$q$ upturn in $I(q)$. The best fit to the data was obtained by Eq. (5), an empirical sum of an Ornstein–Zernicke (OZ) function describing the high-$q$ portion of the data and a Debye–Bueche (DB) function describing the low-$q$ upturn in $I(q)$. The summation of two scattering models in Eq. (5) assumes that the scattering arises from SLD variations at two widely different length scales. The best fit to the USANS data for I-80 is shown in Fig. 5. The correlation lengths determined from the fit were $\xi_{DB} = 28.4$ μm and $\xi_{OZ} = 0.177$ μm. The correlation length associated with porosity in I-80 was by far the largest among the samples studied. In addition, it is interesting that $\xi_{OZ}$ is of the same order of magnitude as $\xi_{TS}$ determined for the samples listed in Table 2. The separation of length scales between $\xi_{DB}$ and $\xi_{OZ}$ ostensibly justifies the assumed summation of the two models.

### 3.4. USANS invariant analysis

The scattering invariant for each gel listed in Table 2 was obtained by numerical evaluation of Eq. (17c) using the TS model to represent the coherent part of $I(q)$ at $q < q_{min}$ and $q > q_{max}$. Closed-form expressions for the first and third integrals in Eq. (17c) exist, but they are algebraically awkward and will not be reproduced here. Evaluation of the integrals by numerical integration was accomplished using commercial math analysis software. For gel I-80, it

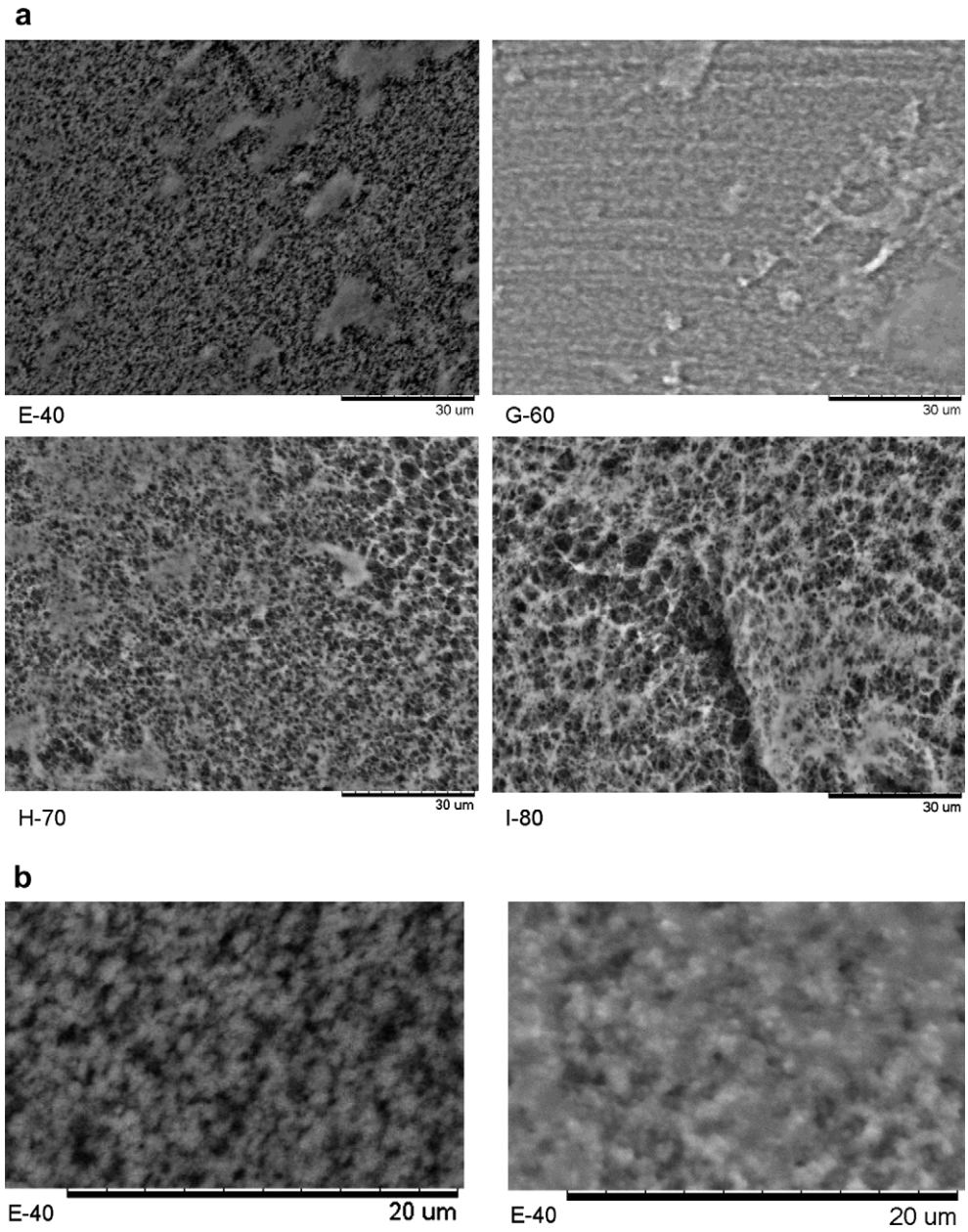


**Fig. 3.** (a) Low-vacuum SEM images of cleaved surfaces of gels E-40, G-60, H-70, and I-80 in a partially hydrated state. (b) Low-vacuum SEM images of gel E-40 in the partly swollen state (left) and air-dried state (right).

was unfortunately not possible to determine the invariant because the OZ function scales as $q^{-2}$ in the high-$q$ limit, such that the third integral in Eq. (17c) does not converge. In addition, a large fraction of the invariant for this sample arises from scattering at $q$ values higher than the measured range. For all other gels, the portion of the invariant derived by integrating the experimental data (over the measured $q$-range) was 60–90% of the total invariant, with the high-$q$ extrapolation accounting for most of the balance. Calculated values of the invariant for the remaining gels are reported in Table 3. Eqs. (16) and (25) were solved simultaneously to obtain values of $\hat{Q}_d$ and $\phi_{1s}$, also reported in Table 3. In the intermediate calculations, the SLD of poly(HEMA) was estimated to be $1.60 \times 10^{-6}$ Å$^{-2}$ from its assumed atomic composition ($C_6H_9DO_3$) and mass density of 1.15 g cm$^{-3}$. The SLD calculation assumed complete H–D exchange between $D_2O$ and the –OH groups of poly(HEMA) after three extractions in $D_2O$. The calculated neutron contrast factor between the $D_2O$-filled pores and the $D_2O$-swollen gel phase ($\Delta\rho_n^2$) and the volume fraction of water in the gel phase ($\phi_{w2}$) are also listed for each gel in Table 3.

The results in Table 3 reveal a few interesting features of the swelling of sponge-like gels. The volume fraction of water in the gel phase at equilibrium is lowest for gel A-00 ($\phi_{w2} = 0.417$), which contained no porogen during crosslinking, and it is highest for gel H-70 ($\phi_{w2} = 0.536$), which had the highest mass fraction of porogen during crosslinking ($w_{PEG} = 0.7$). Therefore, we infer that the effective crosslink density of the gel phase was reduced to some extent by the presence of the porogen. It would not have been correct to evaluate $\phi_{1s}$ for the porous gels from Eq. (16), by assuming that the value of $\hat{Q}_d$ determined gravimetrically for gel A-00 was applicable to the sponge-like gels. A second key observation from Table 3 is that the volume fraction of pores in the swollen state ($\phi_{1s}$) is in all cases less than the mass fraction of porogen during

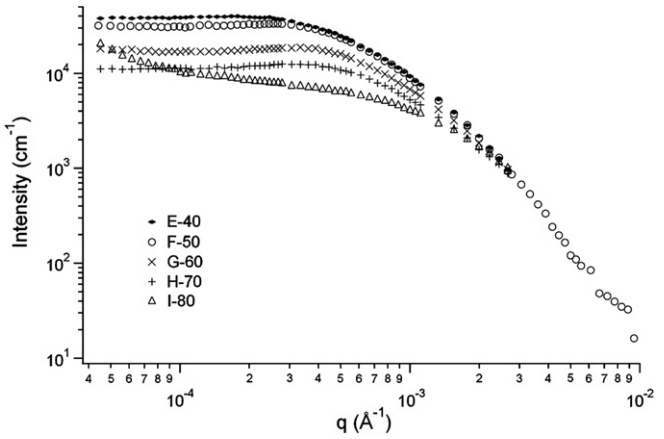


**Fig. 4.** USANS scattering data for swollen porous gels in $D_2O$. Error bars are omitted for clarity.

crosslinking ($w_{PEG}$). While the difference is slight for gel E-40, there is an increasingly large discrepancy as $w_{PEG}$ increases. This trend may be related to the observation that $\phi_{w2}$ is affected by the concentration of the porogen during crosslinking (Table 3). The increased local swelling of the gel phase in samples having high $\phi_{w2}$ may simply force water out of the pores once the porogen is extracted, lowering the value of $\phi_{1s}$.

### 3.5. USANS characterization: dry gels

Additional USANS characterization was conducted to confirm the possible shrinkage or disappearance of the pores after drying, as suggested by the optical transparency of the air-dried gels (Fig. 1) and the low-vacuum SEM images (Fig. 3(b)). For a gel in the dry state that had not been exposed to $D_2O$, an SLD of 0.0 Å$^{-2}$ was assumed for the pore phase, giving $\Delta\rho_n^2 = 1.12 \times 10^{-12}$ Å$^{-4}$ based upon the assumed atomic composition ($C_6H_{10}O_3$). Thus, $\Delta\rho_n^2$ is reduced by approximately a factor of (5–7) compared to similar gels swollen in $D_2O$. Fig. 6 shows raw (uncorrected) scattering data for an empty sample holder, dry gel H-70 in the same sample holder, and swollen gel H-70 in $D_2O$ in the same sample holder. Gel H-70 has a calculated pore phase volume fraction of 0.508 in the swollen state (Table 3). The scattered intensity for the dry gel is statistically indistinguishable from that of the empty cell, except at the low end of the $q$-range, where the lower transmission of the sample suppresses the intensity slightly. The scattered intensity from the dry gel should be lower than that from the $D_2O$-swollen gel due to the different values of $\Delta\rho_n^2$. In the absence of $D_2O$, assuming pores are still present, a factor of (5–7) reduction in $\Delta\rho_n^2$ is expected. However, this reduction is not severe enough to account for the observed disappearance of the coherent scattered intensity in the dry state without assuming a significant reduction in the pore phase volume fraction. Scattering data were also obtained for the other gels in the dry state, with similar results. Based on this evidence, it is reasonable to conclude that the pore phase essentially disappears upon drying.

**Table 2**
Fitted values of the coefficients $a_2$, $c_1$ and $c_2$ of the Teubner–Strey model (Eq. (2)) and the resulting values of the correlation length ($\xi_{TS}$) and the domain size ($d_{TS}$) determined by Eqs. (3) and (4), respectively.

| Sample | $a_2$ (cm) | $c_1$ (cm·Å$^2$) | $c_2$(cm·Å$^4$) | $\xi_{TS}$ (μm) | $d_{TS}$ (μm) |
|---|---|---|---|---|---|
| E-40 | $1.25 \times 10^{-7}$ | 0.413 | $3.66 \times 10^5$ | 0.132 | 6.15 |
| F-50 | $1.85 \times 10^{-7}$ | 0.297 | $4.13 \times 10^5$ | 0.140 | 1.60 |
| G-60 | $2.22 \times 10^{-7}$ | 0.380 | $4.43 \times 10^5$ | 0.119 | 1.20 |
| H-70 | $5.83 \times 10^{-7}$ | 0.474 | $3.66 \times 10^5$ | 0.102 | 1.13 |

**Table 3**
Calculated scattering invariant (Inv), neutron contrast factor ($\Delta\rho_n^2$), pore phase volume fraction ($\phi_{1s}$), gel phase mass swelling ratio in $D_2O$ ($\widehat{Q}_d$), and volume fraction $D_2O$ in the gel phase ($\phi_{w2}$) for porous gels obtained by simultaneous solution of Eqs. (16) and (25).

| Sample | *Inv* (Å$^{-4}$) | $\Delta\rho_n^2$ (Å$^{-4}$) | $\phi_{1s}$ | $\widehat{Q}_d$ | $\phi_{w2}$ |
|---|---|---|---|---|---|
| A-00 | – | – | – | 1.69 | 0.417 |
| E-40 | $3.13 \times 10^{-11}$ | $6.77 \times 10^{-12}$ | 0.370 | 1.82 | 0.458 |
| F-50 | $2.89 \times 10^{-11}$ | $5.15 \times 10^{-12}$ | 0.388 | 1.90 | 0.483 |
| G-60 | $2.37 \times 10^{-11}$ | $4.96 \times 10^{-12}$ | 0.408 | 2.12 | 0.536 |
| H-70 | $2.45 \times 10^{-11}$ | $4.96 \times 10^{-12}$ | 0.508 | 2.13 | 0.537 |

$\widehat{Q}_d$ reported for gel A-00 was determined gravimetrically from swelling measurements in $H_2O$ (Eqs. (7) and (21)).

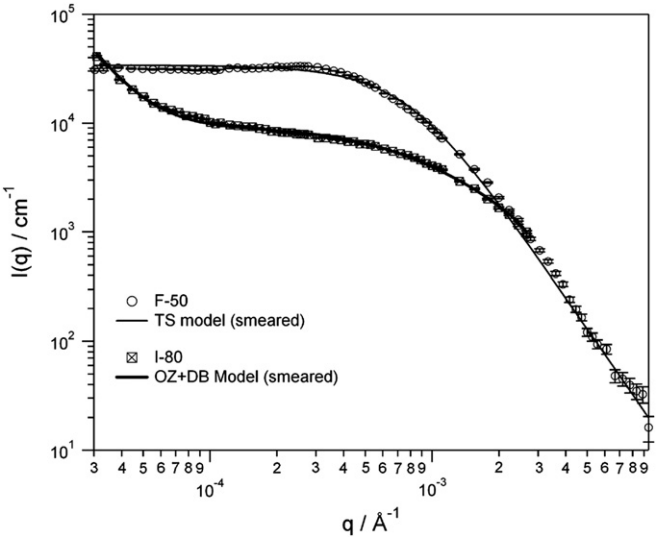


**Fig. 5.** Best fits of slit-smeared scattered intensity to different models for porous gels in $D_2O$. Scattering from sample F-50 was fitted to the Teubner–Strey model (Eq. (2)), and scattering from sample I-80 was fitted to the sum of an Ornstein–Zernicke function and a Debye–Bueche function (Eq. (5)). Models were modified to account for slit-smearing as described in Section 2. Best fit parameters are summarized in Table 2.

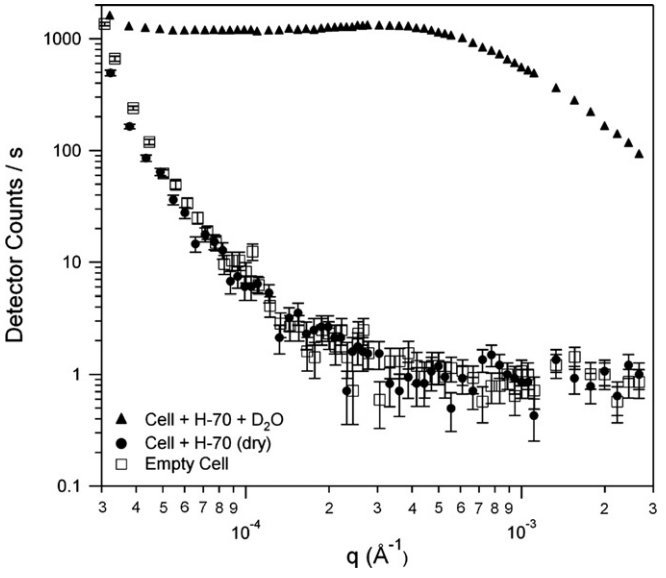


**Fig. 6.** Comparison of raw scattered intensity for $D_2O$-swollen gel H-70, dry gel H-70, and empty cell with quartz windows.

## 4. Summary and conclusions

Neutron scattering invariant analysis and equilibrium swelling measurements can be applied to porous gels to yield the correlation length, the volume fraction of pores, and the concentration of water in the gel phase. The techniques have been demonstrated here for sponge-like hydrogels that have a collapsible pore phase, but the methods are generally applicable to any porous soft material that can be fairly treated as a two-phase system.

An alternative approach to characterize the composition (water content) of the swollen gel phase is the method of neutron contrast variation. The porous gel is swollen in mixtures of $H_2O$ and $D_2O$, allowing determination of the gel phase scattering length density and composition. Contrast variation is frequently applied to characterize pore size and matrix characteristics in porous materials [27–33], but the number of samples that must be characterized for an accurate contrast-match point determination limits its applicability to USANS, where the data collection time required for multiple samples can be prohibitive with currently available instrumentation. The invariant analysis method permits characterization of the pore structure from a single sample. However, limitations of the invariant analysis method include the need to collect data over a wide $q$-range, and the need to identify an acceptable scattering model to extrapolate the data to $q = 0$ and $q = \infty$. Gel I-80 is an example of a material for which the invariant analysis was difficult to apply, for example.

A unique feature of the sponge-like gels studied here is the dramatic shrinkage or collapse of pores during dehydration, which might be driven by surface tension effects. As the water evaporates from the porous gel, the system can lower its total surface energy by decreasing the exposed internal surface area by collapse of the pores. Upon re-hydration, the crosslinking memory effect in the polymer initially encourages the material to return to its reference state at crosslinking. As water plasticizes the material, pores are re-opened. As the gel matrix swells further to equilibrium, the overall dimensions of the gel (and presumably the pores) are again distorted from their reference state at crosslinking.

The swelling of sponge-like gels in a good solvent should, in general, be considered a non-affine deformation. The volume fraction of pores cannot be assumed to be constant during swelling to equilibrium, as illustrated by the expansion of the pore phase in the dry, extracted gels during re-hydration in water. It is also not valid to equate the porogen volume fraction to the pore phase volume fraction at equilibrium. Furthermore, though this study has only reported swelling in water, one cannot safely assume that the pore phase volume fraction is independent of the choice of solvent, as the solvent content in the gel phase likely affects the pore phase volume fraction. Finally, we note that the presence of porogen during crosslinking may affect the chemical architecture of the gel matrix, and therefore alter its equilibrium swelling. The measured water content in the gel phase was dependent on the porogen volume fraction for the sponge-like gels studied here, for example.

## Acknowledgements

This work was supported by the American Chemical Society Petroleum Research Fund under grant #48944-ND7. We acknowledge the support of the National Institute of Standards and Technology, U.S. Department of Commerce, in providing the neutron research facilities used in this work. This work utilized facilities supported in part by the National Science Foundation under Agreement No. DMR-0454672. We thank Prof. Noureddine Abidi and Luis Cabrales of the Fiber and Biopolymer Research Institute, Department of Plant and Soil Science, Texas Tech University, for assisting with obtaining the low-vacuum SEM images.

## References

[1] Hoffman AS. Adv Drug Deliver Rev 2002;54(1):3–12.
[2] Yoshida R. Curr Org Chem 2005;9(16):1617–41.
[3] Kabiri K, Omidian H, Hashemi SA, Zohuriaan-Mehr MJ. Eur Polym J 2003;39(7):1341–8.
[4] Ahn SK, Kasi RM, Kim SC, Sharma N, Zhou YX. Soft Matter 2008;4(6):1151–7.
[5] Savina IN, Cnudde V, D'Hollander S, Van Hoorebeke L, Mattiasson B, Galaev IY. Soft Matter 2007;3(9):1176–84.
[6] Strachotova B, Strachota A, Uchman M, Slouf M, Brus J, Plestil J. Polymer 2007;48(6):1471–82.
[7] Ozmen MM, Okay O. Polymer 2005;46(19):8119–27.
[8] Chern JM, Lee WF, Hsieh MY. J Appl Polym Sci 2004;92(6):3651–8.
[9] Lee WF, Chiu RJ. J Appl Polym Sci 2003;90(8):2214–23.
[10] Kim JH, Lee SB, Kim SJ, Lee YM. Polymer 2002;43(26):7549–58.
[11] Vasilevskaya VV, Khokhlov AR. Macromol Theor Simul 2002;11(6):623–9.
[12] Okay O. Prog Polym Sci 2000;25(6):711–79.
[13] Kulygin O, Silverstein MS. Soft Matter 2007;3(12):1525–9.
[14] Okay O, Gurun C. J Appl Polym Sci 1992;46(3):401–10.
[15] Ceylan D, Okay O. Macromolecules 2007;40(24):8742–9.
[16] Plieva F, Oknianska A, Degerman E, Galaev IY, Mattiasson B. J Bimoat Sci Polym E 2006;17(10):1075–92.
[17] Kato N, Gehrke SH. Colloid Surface B 2004;38(3, 4):191–6.
[18] Lee WF, Lin YH. J Appl Polym Sci 2006;102(6):5490–9.
[19] Lee WF, Yeh YC. J Appl Polym Sci 2006;100(4):3152–60.
[20] Sayil C, Okay O. Polym Bull 2002;48(6):499–506.
[21] Tomotake Y, Maeda Y, Gotoh T, Sakohara S. Kobunshi Ronbunshu 2002;59(1):44–50.
[22] Sayil C, Okay O. Polymer 2001;42(18):7639–52.
[23] Gotoh T, Nakatani Y, Sakohara S. J Appl Polym Sci 1998;69(5):895–906.
[24] Barker JG, Glinka CJ, Moyer JJ, Kim MH, Drews AR, Agamalian M. J Appl Crystallogr 2005;38:1004–11.
[25] Teubner M, Strey R. J Chem Phys 1987;87(5):3195–200.
[26] Horkay F, Hecht AM, Zrinyi M, Geissler E. Polym Gels Netw 1996;4(5, 6):451–65.
[27] Kim MH, Glinka CJ. Micropor Mesopor Mat 2006;91(1–3):305–11.
[28] Hedden RC, Lee HJ, Bauer BJ. Langmuir 2004;20(2):416–22.
[29] Hedden RC, Lee HJ, Soles CL, Bauer BJ. Langmuir 2004;20(16):6658–67.
[30] Silverstein MS, Bauer BJ, Hedden RC, Lee HJ, Landes BG. Macromolecules 2006;39(8):2998–3006.
[31] Vogt BD, Pai RA, Lee HJ, Hedden RC, Soles CL, Wu WL. Chem Mater 2005;17(6):1398–408.
[32] Calo JM, Hall PJ. Carbon 2004;42(7):1299–304.
[33] Ramsay JDF. Adv Colloid Interfac 1998;76:13–37.